

RF and Microwave Electrical Response of Carbon Nanotube Saline Solutions for Potential Biomedical Applications

Mikhail V. Shuba^{1,*}, Gregory Ya. Slepyan¹, Sergey A. Maksimenko¹, and George W. Hanson^{2,*}

¹*Institute for Nuclear Problems, Belarus State University, Bobruiskaya 11, 220030 Minsk, Belarus*

²*Department of Electrical Engineering, University of Wisconsin-Milwaukee, Milwaukee, Wisconsin 53211, USA*

In this study, we present the calculation of effective permittivity of a conductive NaCl solution with embedded singlewall carbon nanotubes (SWCNTs) in the microwave and radio frequency range. We show a strong dependence of the effective suspension permittivity and conductivity on SWCNT length at the same SWCNT volume fraction. The enhancement factor of electromagnetic energy absorption significantly increases with nanotube length. Presented results can be applied for experimental development of therapeutic and diagnostic SWCNT applications, including selective thermolysis of cancer cells and thermoacoustic imaging.

Keywords: Carbon Nanotube, Radiofrequency, Finite Length Effect, Saline, Absorption Enhancement.

Nowadays, carbon nanotubes are considered as perspective thermal contrast agents for microwave and radiofrequency exposing fields.^{1–7} The first experiment on carbon nanotube-enhanced thermal destruction of cancer cells in a radiofrequency field¹ demonstrated a new possibility for cancer treatment of deep tissues. The experimental⁵ and theoretical⁷ studies of singlewall carbon nanotubes (SWCNTs) as thermal contrast agents for microwave detection of breast cancer have also been reported. The theoretical studies of SWCNT-enhanced microwave discrimination of lesions are presented in Ref. [6].

Earlier in Ref. [4] we considered the mechanisms of radiofrequency electromagnetic energy dissipation for different types of individual carbon nanotubes (singlewall and multiwall carbon nanotubes and SWCNT bundles) embedded in a conductive host. In the present paper we theoretically study for the first time the effective dielectric parameters of SWCNT–saline suspensions in the frequency range from 10 MHz to 1 GHz. We compare our theoretical results with experimental data from Ref. [3]. For optimization of possible future experiments on the realization of high electromagnetic energy absorption enhancement, we investigate the dependence of absorption enhancement on SWCNT length.

Let us consider the effective dielectric parameters of a SWCNT suspension in the microwave and radiofrequency

ranges. According to experimental data³ the effective conductivity of the SWCNT suspension linearly increases with increasing SWCNT density from 0 to 1.12 mg/cm³ at frequencies from 20 MHz to 1 GHz. This means that the local fields inside the suspension are small and electromagnetic interaction between the tubes can be neglected. In this case we can apply the Waterman–Truell formula^{8,9} adopted to estimate the relative permittivity of SWCNT suspensions,¹⁰

$$\varepsilon_{\text{eff}}(\omega) = \varepsilon_h(\omega) + \frac{1}{3\varepsilon_0} \sum_j \int_0^\infty \alpha_j(\omega, L) N_j(L) dL \quad (1)$$

where ε_h is relative permittivity of the host media (NaCl solution); $\varepsilon_0 = 8.85 \times 10^{-12}$ F/m; the function $N_j(L)$ describes the number density of SWCNTs of type j , length L and radius R_j ; the factor 1/3 in Eq. (1) is due to the random orientations of the SWCNTs; $\alpha_j(\omega, L)$ is the axial polarizability of an isolated SWCNTs of type j and can be calculated using the integral equation technique described in Ref. [4]. As was shown in Ref. [10], the axial polarizability of all metallic tubes depends slightly on nanotube radius, therefore we did not take variations in radius into account and instead modelled all metallic SWCNTs as being of a single type. For illustrative results, we first took a suspension with two types of inclusions. An inclusion had to be a zigzag SWCNT of one of the following two types: metallic SWCNTs (15, 0) and semiconducting (14, 0). According to the equiprobability of SWCNTs

*Authors to whom correspondence should be addressed.

of identical radii but different chirality in practically available SWCNTs, the ratio of the density of metallic tubes to the density of semiconducting tubes was taken to be equal to 1/2. Although we shall make calculations for a composite of zigzag SWCNTs, all presented results are true for composites with SWCNTs of different chirality. This follows from the fact that the axial surface conductivity [Eq. (24) in Ref. [11]] and axial tube polarizability [Eq. (2) in Ref. [10]] are practically the same for all types of metallic SWCNTs, whether chiral or achiral, of identical radius. The conductivity of small radius (1–3 nm) semiconducting tubes in the microwave and radiofrequency ranges does not depend on the chirality, because it is determined mostly by impurity doping mechanisms in SWCNTs. Therefore we shall describe the semiconducting SWCNTs with only one type zigzag (14, 0) SWCNTs with effective conductivity σ_s (see below).

In all calculations the axial surface conductivity σ_m of metallic SWCNTs was taken using the Drude-law¹¹ with relaxation time 3.3×10^{-14} s (see Ref. [10]). As theoretically shown in Ref. [12] the substitutional doping can lead to the increase of the semiconducting SWCNT conductivity and slight variation of metallic SWCNT conductivity. Existing experiments at high terahertz frequencies¹³ and dc¹⁴ show that the conductivity of semiconducting SWCNTs σ_s is only several orders of magnitude lower than the conductivity of metallic SWCNTs σ_m , rather than the many orders of magnitude expected from Drude theory. This can be explained by impurities and atmospheric oxygen doping in SWCNTs. The value σ_s is an adjustable parameter in our approach, because it can be varied with variation of the technological method of SWCNTs preparation and purification. Comparison of our theoretical results with experimental data of Ref. [3] suggests that the value σ_s should be 470 times lower than the conductivity σ_m of metallic SWCNTs with the same radius. For example, the axial surface conductivity of metallic (15, 0) and semiconducting (14, 0) zigzag SWCNTs were taken in our calculations respectively as

- (i) $\sigma_m = 2.4 \times 10^{-3} + i5.0 \times 10^{-9}$ S and $\sigma_s = 5.1 \times 10^{-6} + i1.1 \times 10^{-11}$ S, at frequency 10 MHz and
- (ii) $\sigma_m = 2.4 \times 10^{-3} + i5.0 \times 10^{-7}$ S and $\sigma_s = 5.1 \times 10^{-6} + i1.1 \times 10^{-9}$ S at frequency 1 GHz.

We shall demonstrate our numerical results in the radio and microwave frequency range from 10 to 1000 MHz. We describe the dielectric properties of NaCl solution in this frequency range with the Cole–Cole relaxation function¹⁵

$$\varepsilon_h(\omega) = \varepsilon(\infty) + \frac{\varepsilon(0) - \varepsilon(\infty)}{1 - (i\omega\tau_w)^{1-\alpha}} + i \frac{\sigma_{\text{sal}}}{\omega\varepsilon_0} \quad (2)$$

The parameters of Eq. (2) were taken from measurement data in Ref. [3] for normal saline (ultrapure water with 0.9% weight/volume of NaCl): $\varepsilon(\infty) = 4.5$, $\alpha = 0.02$, $\varepsilon(0) = 76$, $\tau_w = 8.11 \times 10^{-12}$ s, $\sigma_{\text{sal}} = 1.45$ S/m.

For evaluation of the enhancement of electromagnetic energy absorption due to the addition of SWCNTs in a solution, we introduce a relative absorption rate

$$\theta = \frac{P_s}{P_h} = \frac{\text{Im}[\varepsilon_{\text{eff}}]}{\text{Im}[\varepsilon_h]} \quad (3)$$

where P_s and P_h are the powers dissipated in the SWCNT suspension and in a pure suspension without SWCNTs, respectively. It should be noted that when one introduces a SWCNT into a conducting host medium such as saline, the intense electric field in the host medium in the vicinity of the SWCNT ends causes considerable absorption. This is additional absorption in the host due to the presence of the SWCNT, which must be added to the intrinsic absorption of the SWCNT itself.

In laboratory measurements of solution samples surrounded by air (i.e., solutions housed in a cuvette in a testing chamber), one can assume that heat convection and heat radiation from the suspension can be ignored. In this case, θ is equal to the relative heating rate of the suspension

$$\theta = \frac{\partial T_2 / \partial t}{\partial T_1 / \partial t} \quad (4)$$

where $\partial T_2 / \partial t \propto P_s$ is the heating rate of the SWCNTs suspension and $\partial T_1 / \partial t \propto P_h$ is the heating rate of the solution without SWCNTs. Thus, θ provides the increase in heating due to the addition of the SWCNTs, which is a principle quantity of interest.

Since the SWCNTs in the suspensions considered in Ref. [3] have a range of lengths from 100 to 1000 nm, and the exact distribution functions $N_j(L)$ are not known, we shall restrict consideration to suspensions consisting of SWCNTs having identical length. In order to obtain the real and imaginary relative permittivity to be close to experimental results of Ref. [3], all SWCNTs were taken to be of length $L = 300$ nm, and the volume fraction of all tubes (conceived as cylinders of volume $\pi R_j^2 L$) was $f = \pi \sum_j R_j^2 \int_0^\infty L N_j(L) dL = 4.1 \times 10^{-4}$ that corresponds to carbon density $\rho_c = 1.1$ mg/cm³, which is the same as in experiments.³

The frequency dependence of real and imaginary parts of effective relative permittivity of SWCNT–saline suspension at different SWCNT densities are shown in Figures 1(a) and (b) respectively. The value $\text{Re}(\varepsilon_{\text{eff}})$ slightly varies with frequency and significantly increases with SWCNT density increasing. We found that within the considered frequency range (10 MHz to 1 GHz) the value $\alpha_j(\omega, L)$ for metallic tubes does not depend on the tube conductivity, remaining approximately the same at $\tau > 3.3 \times 10^{-14}$ s. The value α_j for semiconducting tubes varies strongly with variation of tube conductivity. Moreover the value $\text{Re}(\alpha_j)$ for metallic tubes practically does not depend on the frequency in the considered frequency range, whereas the value $\text{Re}(\alpha_j)$ for semiconducting tubes decreases with frequency increasing. Therefore we can

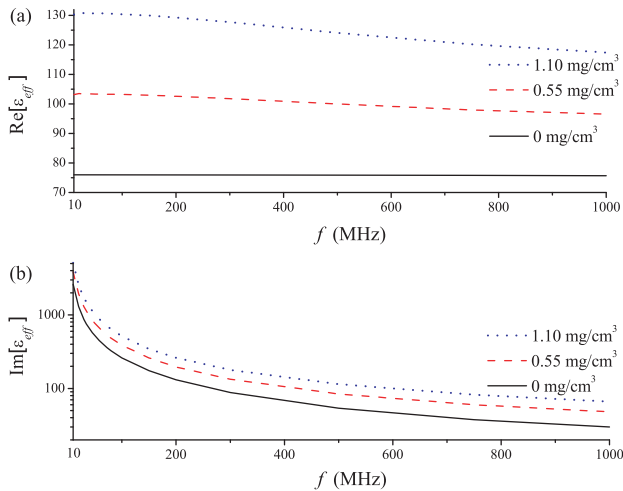


Fig. 1. Frequency dependence of the real (a) and imaginary (b) part of effective relative permittivity ϵ_{eff} of SWCNT-saline suspension at different nanotube densities: 0 mg/cm^3 (solid line), 0.55 mg/cm^3 (dashed line), 1.10 mg/cm^3 (dotted line).

divide the value $\text{Re}(\epsilon_{\text{eff}})$ into three parts: $\text{Re}(\epsilon_{\text{eff}}) = \epsilon'_w + \epsilon'_m + \epsilon'_s$, where $\epsilon'_w(\omega)$ is the real part of relative permittivity of normal saline (solid line in Fig. 1(a)), $\epsilon'_m \cong 35$ is the contribution from the metallic tubes, and $\epsilon'_s(\omega)$ is the contribution from the semiconducting tubes, smoothly varying from 18 (at 10 MHz) to 6 (at 1000 MHz). The contributions of metallic and semiconducting tubes to the value of $\text{Im}(\epsilon_{\text{eff}})$ are approximately identical.

The effective conductivity $\sigma_{\text{eff}} = \epsilon_0 \omega \text{Im}[\epsilon_{\text{eff}}]$ and relative absorption rate θ of the SWCNT suspension at different SWCNT densities are shown in Figures 2(a) and (b) respectively. It should be noted that the data presented in

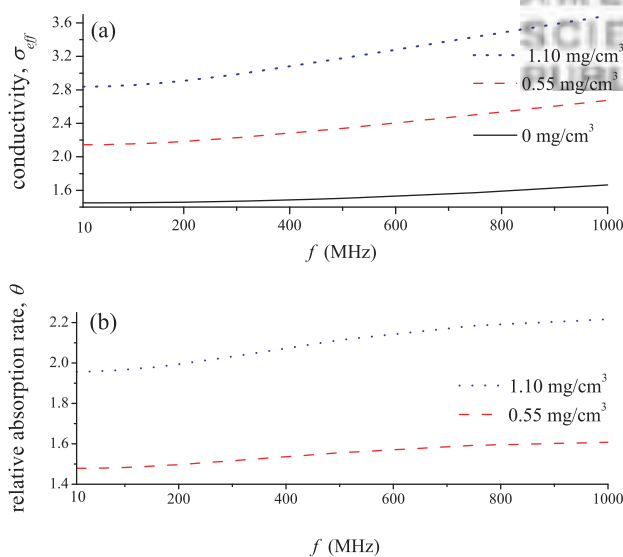


Fig. 2. Frequency dependence of the real part of effective conductivity $\text{Re}(\sigma_{\text{eff}})$ (a) and relative absorption rate of SWCNT-saline suspension at different nanotube densities: 0 mg/cm^3 (solid line), 0.55 mg/cm^3 (dashed line), 1.10 mg/cm^3 (dotted line).

Figures 1 and 2(a) approximately coincide with the experimental data of Ref. [3]. In Ref. [3] 0.02% Pluronic F10 surfactant was added to the SWCNT suspension to prevent SWCNT flocculation. Our calculations do not take into account the pluronic coating of SWCNTs. However, as shown in Ref. [4] the dielectric coating of a SWCNT can enhance the absorption cross section of metallic SWCNTs at low frequency (10 MHz) and slightly change the absorption cross section of metallic SWCNTs at higher frequency (200 MHz). The experimental data in Ref. [3] does not show significant variation of effective suspension conductivity with frequency variation. Therefore, we can conclude that the influence of pluronic coating on the effective dielectric parameters of the suspension is not meaningful in the experiments.

Figure 2(b) demonstrate twofold absorption enhancement in SWCNT-saline suspension with nanotube density 1.1 mg/cm^3 (volume fraction of 4.1×10^{-4}) in the broad frequency range (from 10 MHz to 1 GHz).

Let us now consider the influence of SWCNT length on the effective dielectric parameters of the SWCNT suspension. Figure 3 shows SWCNT length dependence of effective relative permittivity and relative absorption rate θ of the SWCNT-saline suspension at different frequencies and the same SWCNT density. As shown in Figure 3 the values $\text{Re}[\epsilon_{\text{eff}}]$, $\text{Im}[\epsilon_{\text{eff}}]$ and θ significantly increase with tube

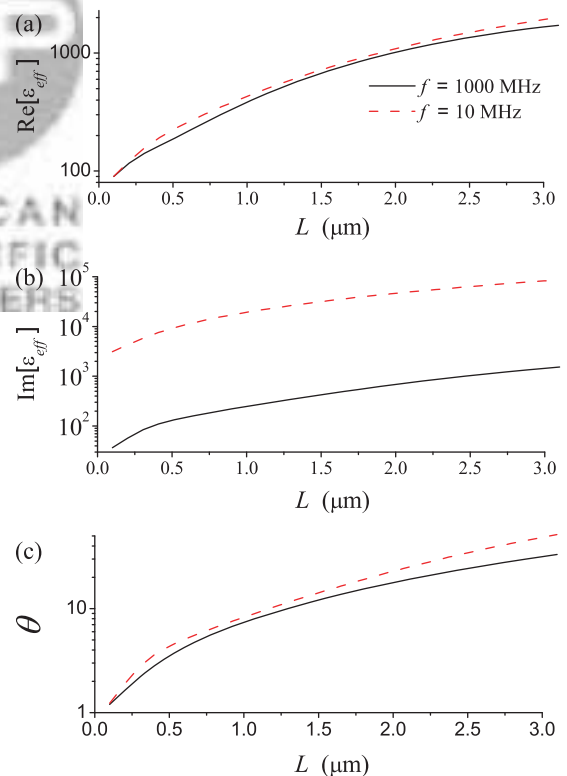


Fig. 3. Frequency dependence of the real (a) and imaginary (b) part of effective relative permittivity and relative absorption rate (c) of SWCNT-saline suspension at different frequency: 10 MHz (dashed line), 1000 MHz (solid line) and the same SWCNT density $\rho_c = 1.12 \text{ mg/cm}^3$.

length increasing. The value $\text{Re}[\varepsilon_{\text{eff}}]$ reaches the value of 2000 at $L = 3 \mu\text{m}$, which is 16 times larger than was obtained in experiments³ (the experiments only considered SWCNTs up to $L = 1000 \text{ nm}$). As shown in Figure 3(c), at frequency 1 GHz the value θ for SWCNTs of length $3 \mu\text{m}$ is 30 times larger than the value θ for SWCNTs of length $0.1 \mu\text{m}$. The reason is the decrease of the importance of the depolarizing field in the metallic SWCNT with increasing length, resulting in an increase in the current in the SWCNT.

Thus we can conclude that the application of longer SWCNTs ($1\text{--}3 \mu\text{m}$) for the enhancement of energy dissipation is more effective than the application of shorter SWCNTs ($0.1\text{--}0.3 \mu\text{m}$), which was also noted in Ref. [2]. The calculation shows that for longer tubes ($0.6\text{--}3 \mu\text{m}$) the contribution of semiconducting tubes to the value of $\text{Re}[\varepsilon_{\text{eff}}]$ is much smaller than the contribution of metallic tubes, whereas the contributions of metallic and semiconducting tubes to the value of $\text{Im}[\varepsilon_{\text{eff}}]$ are comparable with each other. As was shown in Ref. [4], due to the screening effect the application of individual SWCNTs for absorption enhancement is more preferable than application of SWCNTs bundles. We suppose that in the experiments of Ref. [3] the SWCNT suspension contains SWCNTs-bundle together with individual SWCNTs. That is why the authors of Ref. [3] obtained the value $\theta = 2$. Theoretical calculation presented in Figure 3(c) demonstrates that the effective parameters of the SWCNTs suspension can be several times (or even tens of times) larger than that obtain in Ref. [3] if one utilizes suspensions containing only individual, long-length SWCNTs.

In conclusion, we presented for the first time the calculation of effective permittivity and relative absorption rate for SWCNT–saline suspensions taking into account finite-length effects in SWCNTs. The results of calculation are in accordance with the data presented in Ref. [3]. The strong dependence of effective dielectric parameters on SWCNT length is demonstrated. Due to finite length effects in SWCNTs, the application of long-length

individual SWCNTs for absorption enhancement is more preferable than application of short-length SWCNTs. Presented results can be applied for experimental development of therapeutic and diagnostic SWCNT applications, including selective thermolysis of cancer cells and thermoacoustic imaging.

Acknowledgments: This research was partially supported by the Belarus Republican Foundation for Fundamental Research (BRFFR) under projects F10R-002 and F10CO-020, EU FP7 under projects FP7-230778 TERACAN and FP7-266529 BY-NanoERA, and ISTC project B-1708.

References and Notes

1. C. J. Gannon, P. Cherukuri, B. I. Yakobson, L. Cognet, J. S. Kanzius, C. Kittrell, R. B. Weisman, M. Pasquali, H. K. Schmidt, R. E. Smalley, and S. A. Curley, *Cancer* 110, 2654 (2007).
2. G. W. Hanson and S. K. Patch, *J. Appl. Phys.* 106, 054309 (2009).
3. H. M. Gach and T. Nair, *Bioelectromagnetics* 31, 582 (2010).
4. M. V. Shuba, G. Ya. Slepyan, S. A. Maksimenko, and G. W. Hanson, *J. Appl. Phys.* 108, 114302 (2010).
5. A. Mashal, B. Sitharaman, X. Li, P. K. Avti, A. V. Sahakian, J. H. Booske, and S. C. Hagness, *IEEE Trans. on Biomed. Eng.* 57, 1831 (2010).
6. J. D. Shea, P. Kosmas, B. D. V. Veen, and S. C. Hagness, *Inverse Problems* 26, 074009 (2010).
7. Y. Chen, I. J. Craddock, and P. Kosmas, *IEEE Trans. on Biomed. Eng.* 57, 1003 (2010).
8. P. C. Waterman and R. Truell, *J. Math. Phys.* 2, 512 (1961).
9. A. Lakhtakia, *Int. J. Electron.* 75, 1243 (1993).
10. G. Ya. Slepyan, M. V. Shuba, S. A. Maksimenko, C. Thomsen, and A. Lakhtakia, *Phys. Rev. B* 81, 205423 (2010).
11. G. Ya. Slepyan, S. A. Maksimenko, A. Lakhtakia, O. Yevtushenko, and A. V. Gusakov, *Phys. Rev. B* 60, 17136 (1999).
12. A. M. Nemilentsau, M. V. Shuba, G. Ya. Slepyan, S. A. Maksimenko, P. Thomsen, and A. Lakhtakia, *Phys. Rev. B* 82, 235424 (2010).
13. C. Beard, J. L. Blackburn, and M. J. Heben, *Nano Lett.* 8, 4238 (2008).
14. X. Zhou, J.-Y. Park, S. Huang, J. Liu, and P. L. McEuen, *Phys. Rev. Lett.* 95, 146805 (2005).
15. C. Gabriel and A. Peyman, *Phys. Med. Biol.* 51, 6003 (2006).

Received: 3 January 2011. Accepted: 24 May 2011.